Hybrid Nanomaterials

DOI: 10.1002/anie.201200409

Hybrid Nanomaterials that Mimic the Food Effect: Controlling Enzymatic Digestion for Enhanced Oral Drug Absorption**

*Angel Tan, Amanda Martin, Tri-Hung Nguyen, Ben J. Boyd, and Clive A. Prestidge**

Lipid-based, colloidal systems are a platform for encapsulation technology in therapeutic and nutraceutical research for mimicking the food effect. A positive food effect takes place when the bioavailability of poorly water-soluble, lipophilic therapeutics and vitamins increases significantly (by at least 25%) when co-administered with high-fat meals.[1] Lipid-based dosage forms have evolved from simple lipid solutions, suspensions, and macroemulsions,[2] to the more complex lipid-based nanovectors, such as self-micro/nanoemulsifying drug delivery systems (SM/NEDDS), solid lipid nanoparticles (SLN), polymeric micelles, and vesicular carriers (e.g. liposomes, niosomes) with "smart" surface coatings.[1b,3] These colloidal structures are formed based on self-assembly of amphiphilic molecules, in which the lipophilic moieties effectively host and prevent precipitation of the active compounds, thereby facilitating their transportation towards the absorptive sites in the stomach or intestines. Recent advances in these lipid-based systems have been optimizing the carrier targetability to the site of absorption or drug action (e.g. lymphatic uptake for localized treatment),[4] as well as their transformation from the conventional liquid state into solid-dosage forms.[5]

Drug release from lipid nanovectors is known to involve two major mechanisms. One mechanism is concentration-gradient-driven diffusion, in which the drug-release kinetics depend closely on the carrier wettability and surface area; the other mechanism involves degradation of the carrier matrix, wherein the susceptibility of lipid carriers to digestion is modulated by the interfacial binding affinity of digesting enzymes to the lipid substrates.[6] It has been proposed that selective carrier breakdown and drug release within the gastrointestinal tract (i.e. stomach, small intestine, colon) could be achieved with surface-functionalized and structured, emulsion-based systems.[7] Structured, lipid colloidal systems can be fabricated based on different types of particles (e.g. oil droplets, solid lipid particles, hydrogel particles) and different processing operations (e.g. interfacial layer-by-layer coating or cross-linking, and particle or droplet core-filling). In practice, precise control over the enzymatic degradation of various lipid colloidal systems is challenging and research in this area is in its infancy.[7b] The effect of particle size on lipid digestibility and drug absorption is a controversial topic; some studies showed increased lipid digestibility and drug bioavailability with reduced carrier particle sizes,[8] while others reported negligible enhancement.[9] The extent of the food effect contributed by various lipid-dosage forms has been ambiguously drug-specific and mostly unpredictable.[10] This unpredictability represents the greatest barrier for successful translation of these systems from the bench-top to the clinic.

On this basis, we aim to develop functional nanomaterials that mimic the food effect in a predictable manner for achieving better-controlled, therapeutic release and response. Herein, we demonstrate the use of silica nanoparticles of different sizes and porosities to construct specific nanostructured networks to manipulate the enzymatic digestion of colloidal lipids. We present a novel, dual-fluorescence approach for characterizing the internal structure of the nanoparticle–lipid hybrid microparticles, as well as the application of these hybrid carriers to increase the food effect, leading to optimized drug pharmacokinetics.

Using a bottom-up approach (Figure 1), hybrid microparticles composed of silica nanoparticles:colloidal lipids (1:2 w/w) were prepared from precursor Pickering emulsions based on nanoparticle and lipid colloid self-assembly.[11] Tri-/di-/monoglyceride oil droplets (containing the lipophilic guest molecule, celecoxib) were emulsified with soybean lecithin and reduced to submicron emulsions with an average diameter of 200 nm using piston-gap high-pressure homogenization. Interfacial nanoparticle adlayers were formed based on two different types of silica nanoparticles: a) mesoporous Aerosil fumed silica, that is, 50 nm nanoaggregates composed of primary particles of 7 nm with a specific surface area (S_{BET}) of approximately 380 m^2g^{-1}, and b) non-porous Ludox colloidal silica, characterized by an average particle size of 22 nm and S_{BET} of approximately 140 m^2g^{-1}. The adsorption of silica nanoparticles at the oil–water interface is mainly driven by their attraction to the PO_2^--$N(CH_3)_3^+$ dipoles of the phospholipid polar groups.[12] Controlled spray-drying effectively transformed the submicron Pickering emulsions into microparticles with a solid-state, silica–lipid hybrid network composed of internal nanoporous matrices.[11] X-ray powder diffraction analysis (Figure 1) confirmed that the model

[*] Dr. A. Tan, A. Martin, Prof. C. A. Prestidge
Ian Wark Research Institute, University of South Australia
Mawson Lakes, South Australia 5095 (Australia)
E-mail: clive.prestidge@unisa.edu.au
Homepage: http://unisa.edu.au/iwri/staffpages/cliveprestidge.asp
Dr. T.-H. Nguyen, Prof. B. J. Boyd
Monash Institute of Pharmaceutical Sciences, Monash University, Parkville Campus
381 Royal Parade, Parkville, Victoria 3052 (Australia)

[**] We acknowledge the Australian Research Council, the Australian National Health and Medical Research Council, Itek Pty. Ltd. and BioInnovation SA for research funding; Dr. Mihail Popescu and A/Prof. Robert Milne for providing instructive advice on lipolysis data modelling; and Prof. Christopher J. H. Porter for guidance in the pharmacokinetic studies.

Supporting information for this article is available on the WWW under http://dx.doi.org/10.1002/anie.201200409.

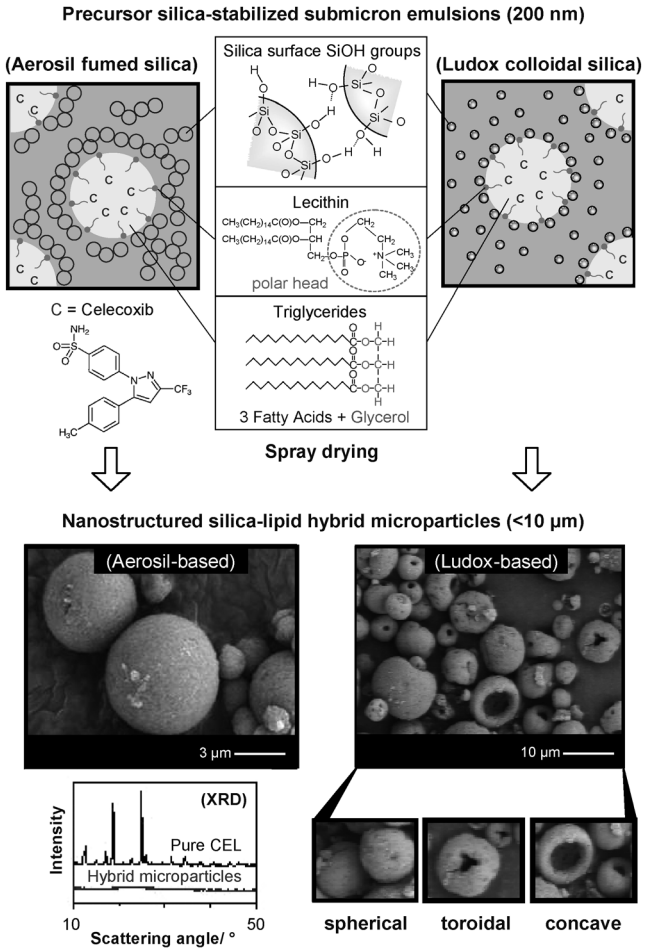

Figure 1. Formation of nanostructured silica–lipid hybrid microparticles of different morphologies from submicron emulsions encapsulated by two different types of silica nanoparticles (gray spheres = nanoparticles, large white circles = lipid). Left: mesoporous, Aerosil fumed silica and right: non-porous, Ludox colloidal silica. Lower images are high-resolution scanning electron microcopy images. X-ray powder diffraction (XRD) shows that celecoxib (CEL, 4% w/w as determined using high performance liquid chromatography) was encapsulated in a noncrystalline state in the hybrid microparticles.

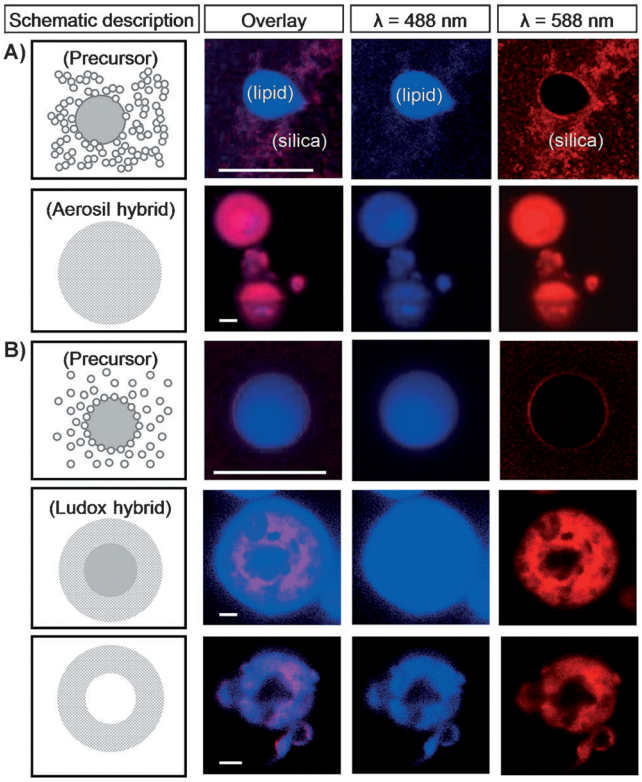

Figure 2. Confocal laser scanning microscopy (CLSM) cross section images of the hybrid microparticles and their precursor emulsions stabilized by A) mesoporous Aerosil fumed silica and B) non-porous Ludox colloidal silica (scale bars = 1 μm). Lipid = blue field, silica = red field. Schematic representations: gray = lipid, small circles = nanoparticles, hatching = lipid–nanoparticle hybrid material.

drug, celecoxib (log $P = 3.5$, p$K_a = 11.1$), was encapsulated in a noncrystalline form in the silica–lipid matrices for at least 12 months when stored at ambient conditions.

The morphology and internal nanostructure of the hybrid microparticles were shown to be controllable by the porosity of the outer silica nanoparticles. High-resolution scanning electron microscopy showed that at a silica:lipid ratio of 1:2 (w/w), mesoporous, Aerosil silica produced spherical, enclosed structures, whereas non-porous, Ludox silica formed a mixture of spherical and non-spherical particles, including toroidal and concave structures (Figure 1). These spray-dried microparticles and the corresponding precursor emulsions were further analyzed for their internal structures and chemical homogeneity using confocal microscopic imaging of the fluorescently labeled droplets and nanoparticles (Figure 2). The Aerosil-based precursor emulsions were visualized as sparsely coated droplets with extensive silica-nanoparticle bridging between neighboring lipid droplets in the continuous phase (Figure 2 A). In contrast, Ludox-based precursor emulsions appeared to be more densely encapsulated by the nanoparticle adlayer at the interface (Figure 2 B). The Ludox silica particles (less than one SiOH group per nm^2) were better dispersed in water than the Aerosil silica particles, which remained flocculated in water (through hydrogen bonding) mainly because of their higher surface silanol content (i.e. 2.5 SiOH groups per nm^2). Spray-drying subsequently induced redistribution of the silica nanoparticles from the water phase into the less-polar, dispersed-lipid phase because of evaporation-driven clustering. This redistribution effectively produced porous microparticles with different interior architectures. As illustrated by the confocal fluorescence images, the Aerosil-based, spherical microparticles were composed of chemically homogenous, silica–lipid hybrid matrices (Figure 2 A); in the case of the Ludox-based microparticles, the resultant toroidal/concave/spherical hybrids were composed of core–shell structures with or without an oil interior, enclosed by a porous shell (Figure 2 B). All of these porous hybrid structures were easily re-dispersed in aqueous media with particle sizes of 5 μm or smaller, as determined using laser diffraction analysis (Supporting Information, Figure S1). The Brunauer–Emmett–Teller surface area (S_{BET}) and Barrett–Joyner–Halenda (BJH) average pore width ($4\,V/S_{BET}$) of the lipid-extracted microparticles were

determined to be 184 $m^2 g^{-1}$ and 3 nm for the Aerosil hybrids; and 66 $m^2 g^{-1}$ and 7 nm for the Ludox hybrids.

The specific nanostructures of the hybrid microparticles were shown to significantly influence the digestibility of the encapsulated lipid colloids, in comparison with conventional (unencapsulated) lipid solutions and emulsions. The lipid-digestion profiles were investigated under simulated, intestinal conditions using a pH-stat titrimetric method, which monitors the extent of lipid ester-linkage hydrolysis, based on the production of free fatty acids from each tri-/di-/monoglyceride molecule in the presence of pancreatin extracts.[13] The enzyme-mediated lipid hydrolysis process can be described as a pseudo-first-order reaction [Eq. (1)] because the reaction rate is strongly dependent on the concentration of the lipid substrates, whereas the concentration (i.e. activity) of the lipid-digesting enzymes is expected to remain constant throughout the reaction due to their presence in excess:

$$[\text{lipolysis products}] = k_0[\text{lipids}][\text{enzymes}] = k[\text{lipids}] \quad (1)$$

where k_0 is the first-order reaction rate constant, and $k = k_0[\text{enzymes}]$ is the pseudo first-order reaction rate constant. The lipolysis processes were determined to be mono-, bi-, or tri-phasic reactions depending on the types of lipid system.[6c] The mono-, bi-, or tri-exponential equations [Eq. (2)] were fitted to the lipolysis data using an iterative curve stripping technique:[14]

$$\%\ \text{lipolysis} = 100-(L_1 e^{-k_1 t} + L_2 e^{-k_2 t} + L_3 e^{-k_3 t}) \quad (2)$$

where L_1, L_2, and L_3 represent the percentages of lipids undergoing lipolysis at a rate constant of k_1, k_2, and k_3, respectively, at time, t.

The coarse oil solution was found to be digested at a relatively low rate constant of 0.04 min^{-1}, whereas the hybrid microparticles significantly enhanced the digestibility of the encapsulated lipids (Figure 3). The mixed core–shell and non-spherical Ludox hybrids produced a more sustained rate of lipid hydrolysis (i.e. 25% of lipids undergo hydrolysis with a rate constant of 1.20 min^{-1}) than the matrix-structured, spherical Aerosil hybrids (i.e. 55% of lipids undergo hydrolysis with a higher rate constant of 2.08 min^{-1}). The increased lipid digestibility promoted by the microparticles is related to the surface area of the microparticle which is increased by their nanopores (i.e. S_{BET} of spherical matrix > spherical core–shell/toroid/concave). The silica nanostructured network acts as a substrate–enzyme immobilization template for facilitating the hydrolytic activity of the interfacially active enzymes.[15] Under physiological conditions, complete intestinal absorption of fat typically occurs at 66% fatty acid release from a fat substrate, where the digested glycerides are absorbable across the intestinal membrane in the form of monoglycerides and fatty acids.[16] It is thus reasonable to consider the time taken for approximately 66% lipid hydrolysis for each system to estimate the rate of drug release (and therefore the bioavailability ranking). The rate could be ranked in the following order: Aerosil hybrid microparticles (4 min) > Ludox hybrid microparticles (12 min) > coarse lipid solution (25 min). It is noteworthy that the lipid digestion performances of both hybrid microparticles were reproducible when tested over a period of 6 months. This situation is different from that of the liquid-state homogenized submicron emulsions, which exhibited variable and unpredictable lipolysis profiles within a week after preparation, mainly attributed to thermodynamic instability of the bare liquid emulsions (Supporting Information, Figure S2).

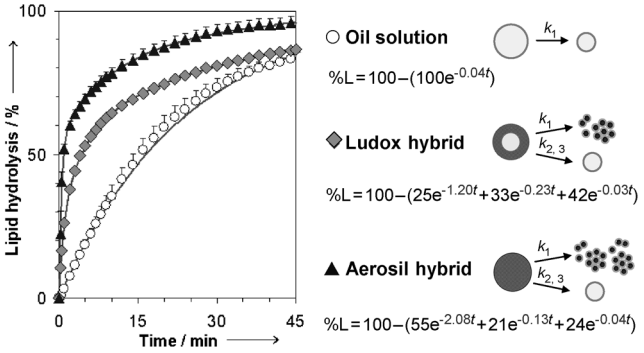

Figure 3. Enzyme-mediated lipid digestion profiles of various lipid-based drug carriers under simulated human fasted-state intestinal conditions at 37°C (mean ± standard error, $n = 3$). The experimental data (symbols) and modeling data (lines) are shown. Right: Light gray sphere = lipid, dark gray sphere = lipid–nanoparticle hybrid.

To confirm our prediction of superior drug-delivery performance of the hybrid microparticles from enhanced lipid digestion, a number of these lipid colloid systems were evaluated for drug absorption performance in beagle dogs. These systems have previously been evaluated using fasted rat models;[11b,17] however, rats are not ideal models for evaluating fed versus fasted state variations, because, unlike humans, rats do not possess a gallbladder, therefore bile secretion in rats is independent of oral lipid intake. The current single oral dose study was conducted at a fixed dose of 3 $mg\,kg^{-1}$ of celecoxib filled into gelatin capsules. The pure celecoxib material was administered under both fed and fasted states for demonstrating the ordinary food effect on its absorption. Two specific pharmacokinetic parameters were evaluated, that is, the relative bioavailability *(F)* with reference to the pure drug (under fasting condition), and the maximum plasma concentration (C_{max}) achieved after dosing. The pharmacokinetic parameters (Figure 4) indicated an approximately threefold increase in the drug absorption when it was administered with fat-rich food. This positive food effect was further enhanced by the Aerosil hybrid microparticles up to 6.5-fold (i.e. two times higher than the fed-state bioavailability), even though the lipid dose for the hybrid microparticles (< 1 g) was much lower than the fat content present in the food (approximately 35 g). This increment is higher than those reported to date for celecoxib in dogs and humans.[9a,18] In agreement with the lipid digestibility ranking, the nanostructured hybrid microparticles were more efficient than the conventional oil solution (also < 1 g lipid dose) in elevating the drug bioavailability. This clearly demonstrates the role of the nanostructured silica network in facilitating lipid processing, which leads to more efficient formation of the micellar phases that keep the released drugs solubilized (depicted in Figure 4). One of our previous absorption studies conducted

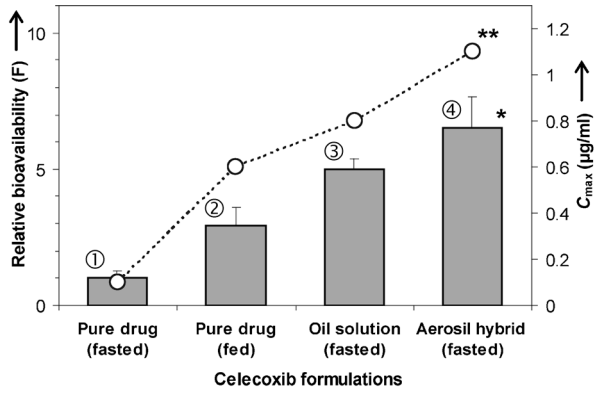

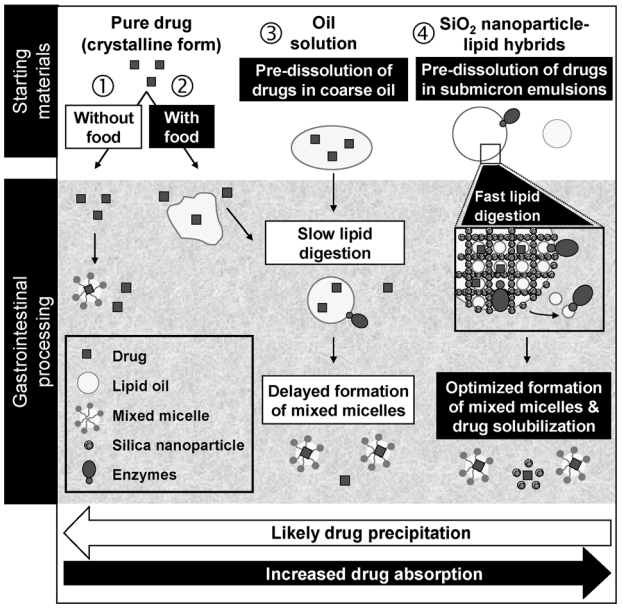

Figure 4. Pharmacokinetic parameters of celecoxib in male beagle dogs following a single oral dose of various formulations equivalent to a celecoxib dose of 3 mg kg^{-1} (mean ± standard error, $n = 4$): relative bioavailability (bars, left axis) and maximum plasma concentration (circles, right axis). (* denotes $p < 0.05$ in comparison with the pure drug in fasted state; ** denotes $p < 0.05$ in comparison with the pure drug in both fed/fasted states and oil solution in fasted state). The schematic diagram depicts the potential gastrointestinal processing pathways for each of the systems (labeled ① to ④ in the histogram; Supporting Information, Figure S3).

in rats also showed the superiority of such hybrid microparticles in enhancing drug bioavailability, in comparison with an unencapsulated submicron emulsion, which is also quickly digested.[11b] These findings indicate that hydrophilic silica nanoparticles may play an additional role as a "precipitation inhibitor" for solubilizing drugs at a supersaturated state in the gastrointestinal lumen, which is a driving force for intestinal drug permeation.[19]

In summary, we have demonstrated the use of nanostructured hybrid microparticles in enhancing the oral absorption of compounds with poor water solubility using an interaction between the lipid-nanoparticle hybrid and the enzymes. The morphology and the internal nanostructure data emphasized that the hybrid microparticles are fundamentally different from the conventional nanoparticle-encapsulated droplets. It is possible to control the external and internal architecture of the hybrid microparticles by using silica nanoparticles of varying sizes and porosities. We hypothesize that the formation of toroidal, concave, and spherical particles can be manipulated by varying the concentration ratio of nanoparticles/lipids, which result in different particle redistribution and encapsulation patterns after drying. Importantly, in vivo studies in dogs clearly show that the nanostructured hybrid microparticles produced significantly higher drug bioavailability in comparison with dietary fats and readily emulsified lipid systems. The ability to enhance and control the digestion of lipid-based nanovectors will enable us to more selectively control the retention, release, and absorption of the encapsulated materials under physiological conditions. These hybrid nanomaterials with engineered biological functions potentially form the basis for the next generation of medicines and functional foods.

Experimental Section

Materials: Celecoxib (≥ 99.0 % purity) was supplied by Chem-Pacific (USA). Miglyol 812 (saturated C_8/C_{12} triglycerides; Hamilton Laboratories, Australia), and Capmul MCM (C_8/C_{12} mono/diglyceride blend; a gift from Abitech Corporation, USA), were used as the emulsion lipid phases. Soybean lecithin (> 94 % phosphatidylcholine, < 2 % triglycerides) was obtained from BDH Merck (Australia). Aerosil 380 silica nanoparticles were purchased from Evonik Degussa (Germany), Ludox TM-40 silica nanoparticles and porcine pancreatin extract (activity equivalent to 8 × USP specification) were from Sigma–Aldrich (Australia).

Hybrid nanomaterial preparation: Precursor emulsions were homogenized (Avestin EmulsiFlex-C5, Canada) under a pressure of 1000 bar for five volume cycles. An aqueous dispersion of 5 % w/v silica nanoparticles was added to the homogenized emulsions and equilibrated for 12 h. The silica-stabilized emulsions were then spray-dried using a BÜCHI Mini Spray Dryer B-290 (Switzerland) using the following parameter settings: emulsion flow rate 5 mL min^{-1}, aspirator setting 100 %, air flow rate 0.6 m^3 min^{-1}, and inlet/outlet temperature at 180/65 °C. The lipid and drug content were determined using thermogravimetric and high performance liquid chromatography (HPLC) analysis (Supporting Information, Table S1), respectively.[11b] Nitrogen gas adsorption measurements were performed for the spray-dried microparticles after the lipid content was extracted with hexane and filter-dried, using a Micromeritics Gemini 2390 BET surface area and porosity analyzer. For confocal fluorescence imaging (Leica TCS-SP5, Germany), the silica nanoparticles were labeled with Rhodamine B (hydrophilic) while the oil phase with Coumarin 102 (lipophilic); these were detected as red and blue images at the emission wavelengths of 588 and 488 nm, respectively (with the corresponding excitation wavelengths of 514 and 405 nm).

Lipid digestion: Mixed micelles consisting of 5:1.25 mM of sodium taurodeoxycholate/phospholipids were used to simulate the human fasted-state intestinal conditions. Each lipid system at a dose of 200 mg oil per 20 mL medium was digested in the presence of 1000 tributyrin units mL^{-1} of porcine pancreatin extract. The progress of lipid digestion was monitored by using a TitraLab 854 pH-stat titration apparatus (Radiometer Analytical, France). Lipid hydrolysis was quantified based on the consumption of NaOH during the titration of free fatty acids produced.

Animal study: The bioavailability study was conducted according to the guidelines of the Institutional Ethics Committee (Melbourne). Four male beagle dogs weighing between 12–16 kg were used in the

four-treatment, four-way, cross-over study with a 7 day washout period. The fed treatment group was given 700 g of commercial dog food (containing $\leq 5\%$ w/w crude fat) 1 h prior to dosing, whereas the fasted treatment groups were fasted for 24 h pre-dose and 10 h post-dose. Blood samples were collected from the cephalic vein using an indwelling catheter at the designated time intervals and analyzed for drug content in the plasma using HPLC.

Received: January 16, 2012
Revised: March 6, 2012
Published online: April 13, 2012

Keywords: drug delivery · emulsions · lipid digestion · nanoparticles · nanostructures

[1] a) C. J. H. Porter, W. N. Charman, *Adv. Drug Delivery Rev.* **2001**, *50*, S127 – S147; b) D. Shukla, S. Chakraborty, S. Singh, B. Mishra, *Expert Opin. Drug Delivery* **2011**, *8*, 207 – 224; c) C. J. H. Porter, N. L. Trevaskis, W. N. Charman, *Nat. Rev. Drug Discovery* **2007**, *6*, 231 – 248.

[2] N. A. Armstrong, K. C. James, *Int. J. Pharm.* **1980**, *6*, 195 – 204.

[3] E. Soussan, S. Cassel, M. Blanzat, I. Rico-Lattes, *Angew. Chem.* **2009**, *121*, 280 – 295; *Angew. Chem. Int. Ed.* **2009**, *48*, 274 – 288.

[4] S. Cai, Q. Yang, T. R. Bagby, M. L. Forrest, *Adv. Drug Delivery Rev.* **2011**, *63*, 901 – 908.

[5] V. Jannin, J. Musakhanian, D. Marchaud, *Adv. Drug Delivery Rev.* **2008**, *60*, 734 – 746.

[6] a) G. Pieroni, R. Verger, *J. Biol. Chem.* **1979**, *254*, 10090 – 10094; b) T. Tsujita, H. Takaichi, T. Takaku, T. Sawai, N. Yoshida, J. Hiraki, *J. Lipid Res.* **2007**, *48*, 358 – 365; c) A. Tan, S. Simovic, A. K. Davey, T. Rades, B. J. Boyd, C. A. Prestidge, *Mol. Pharm.* **2010**, *7*, 522 – 532.

[7] a) D. J. McClements, Y. Li, *Adv. Colloid Interface Sci.* **2010**, *159*, 213 – 228; b) D. J. McClements, *J. Food Sci.* **2010**, *75*, R30 – R42.

[8] a) B. D. Tarr, S. H. Yalkowsky, *Pharm. Res.* **1989**, *6*, 40 – 43; b) P. C. De Smidt, M. A. Campanero, I. F. Trocóniz, *Int. J. Pharm.* **2004**, *270*, 109 – 118.

[9] a) H. Takeuchi, H. Sasaki, T. Niwa, T. Hino, Y. Kawashima, K. Uesugi, H. Ozawa, *Chem. Pharm. Bull.* **1991**, *39*, 3362 – 3364; b) M. Armand, B. Pasquier, M. André, P. Borel, M. Senft, J. Peyrot, J. Salducci, H. Portugal, V. Jaussan, D. Lairon, *Am. J. Clin. Nutr.* **1999**, *70*, 1096 – 1106; c) C. J. H. Porter, A. M. Kaukonen, B. J. Boyd, G. A. Edwards, W. N. Charman, *Pharm. Res.* **2004**, *21*, 1405 – 1412.

[10] D. G. Fatouros, D. M. Karpf, F. S. Nielsen, A. Mullertz, *Ther. Clin. Risk Manage.* **2007**, *3*, 591 – 604.

[11] a) S. Simovic, P. Heard, H. Hui, Y. Song, F. Peddie, A. K. Davey, A. Lewis, T. Rades, C. A. Prestidge, *Mol. Pharm.* **2009**, *6*, 861 – 872; b) A. Tan, S. Simovic, A. K. Davey, T. Rades, C. A. Prestidge, *J. Controlled Release* **2009**, *134*, 62 – 70; c) S. Simovic, T. J. Barnes, A. Tan, C. A. Prestidge, *Nanoscale* **2012**, *4*, 1220 – 1230.

[12] D. A. Pink, M. Belaya, V. Levadny, B. Quinn, *Langmuir* **1997**, *13*, 1701 – 1711.

[13] L. Sek, C. J. H. Porter, W. N. Charman, *J. Pharm. Biomed. Anal.* **2001**, *25*, 651 – 661.

[14] A. Mirfazaelian, M. Mahmoudian, *Biopharm. Drug Dispos.* **2006**, *27*, 119 – 124.

[15] a) A. A. Vertegel, R. W. Siegel, J. S. Dordick, *Langmuir* **2004**, *20*, 6800 – 6807; b) J. C. Cruz, P. H. Pfromm, M. E. Rezac, *Process Biochem.* **2009**, *44*, 62 – 69.

[16] F. Carrière, E. Rogalska, C. Cudrey, F. Ferrato, R. Laugier, R. Verger, *Bioorg. Med. Chem.* **1997**, *5*, 429 – 435.

[17] A. Tan, A. K. Davey, C. A. Prestidge, *Pharm. Res.* **2011**, *28*, 2273 – 2287.

[18] a) S. K. Paulson, M. B. Vaughn, S. M. Jessen, Y. Lawal, C. J. Gresk, B. Yan, T. J. Maziasz, C. S. Cook, A. Karim, *J. Pharmacol. Exp. Ther.* **2001**, *297*, 638 – 645; b) Y. Shono, E. Jantratid, N. Janssen, F. Kesisoglou, Y. Mao, M. Vertzoni, C. Reppas, J. B. Dressman, *Eur. J. Pharm. Biopharm.* **2009**, *73*, 107 – 114.

[19] a) H. R. Guzmán, M. Tawa, Z. Zhang, P. Ratanabanangkoon, P. Shaw, C. R. Gardner, H. Chen, J.-P. Moreau, O. Almarsson, J. F. Remenar, *J. Pharm. Sci.* **2007**, *96*, 2686 – 2702; b) J. Brouwers, M. E. Brewster, P. Augustijns, *J. Pharm. Sci.* **2009**, *98*, 2549 – 2572.

